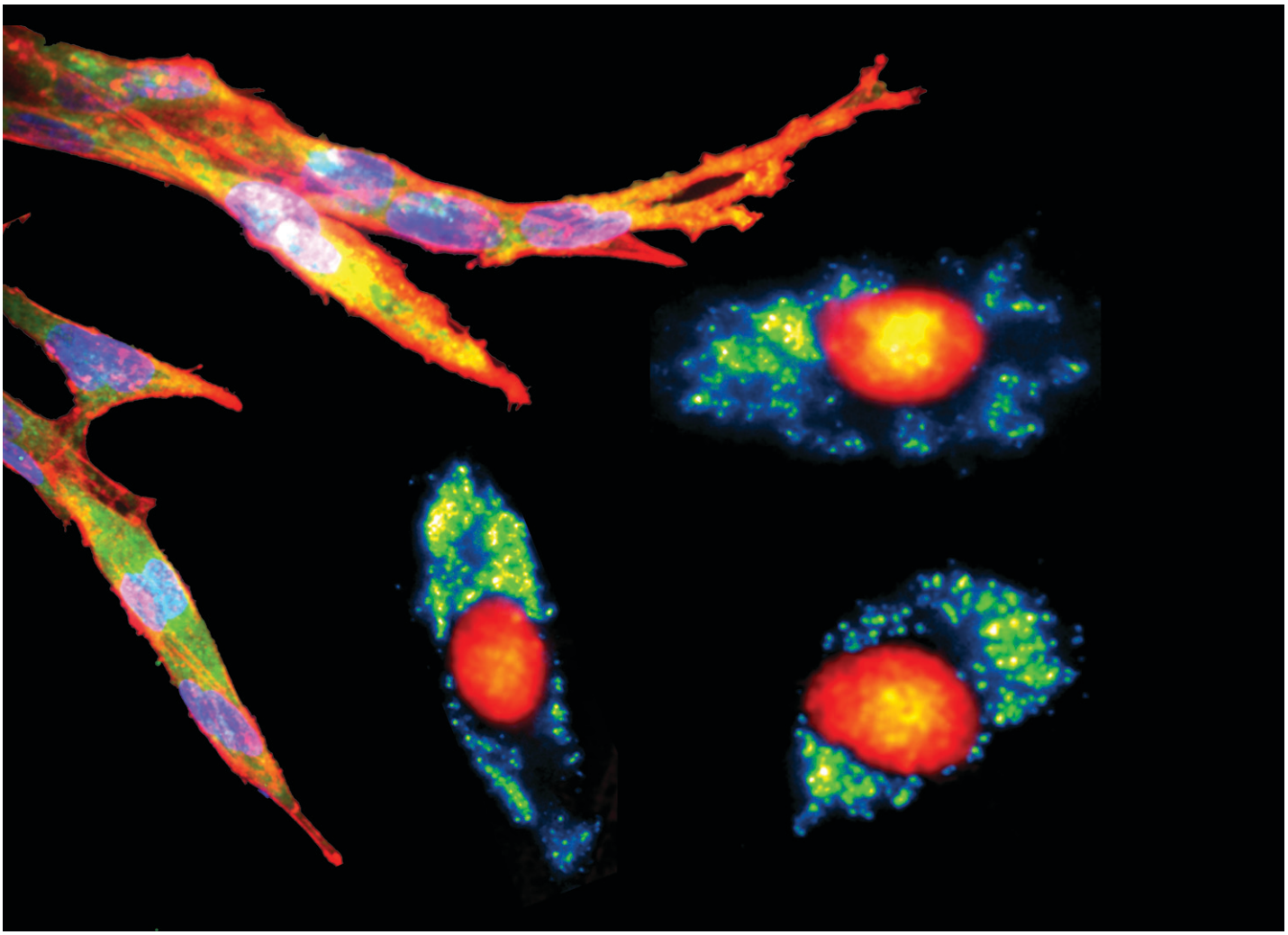

Featuring work from the Department of Mechanical Engineering, Prof. Jianping Fu and Prof. Allen Liu, University of Michigan. Fu lab specializes in mechanobiology and biomimetic tools, Liu lab focuses on mechanotransduction and synthetic biology.

The role of Notch signaling in regulating angiogenic morphogenesis was investigated using a microengineered biomimetic system and a GNR-LNA nanobiosensor. Inhibition of Notch signaling resulted in overexpression of Dll4 mRNA in tip cells and hyper-sprouting endothelial structures.

Notch signaling in regulating angiogenesis in a 3D biomimetic environment

As featured in:

See Allen P. Liu, Jianping Fu *et al.*, *Lab Chip*, 2017, **17**, 1948.

ROYAL SOCIETY OF CHEMISTRY

rsc.li/loc

Registered charity number: 207890

Lab on a Chip

PAPER

View Article Online
View Journal | View Issue

Cite this: *Lab Chip*, 2017, **17**, 1948

Notch signaling in regulating angiogenesis in a 3D biomimetic environment†

Yi Zheng, ‡[a] Shue Wang,‡[a] Xufeng Xue,[a] Alan Xu,[a] Wei Liao,[b] Alice Deng,[c] Guohao Dai,[d] Allen P. Liu *[aefg] and Jianping Fu*[aeh]

Received 22nd February 2017,
Accepted 22nd April 2017

DOI: 10.1039/c7lc00186j

rsc.li/loc

Angiogenesis is a complex cellular process involving highly orchestrated invasion and organization of endothelial cells (ECs) in a three-dimensional (3D) environment. Recent evidence indicates that Notch signaling is critically involved in regulating specialized functions and distinct fates of ECs in newly formed vasculatures during angiogenesis. Here, we demonstrated, for the first time, the application of a microengineered biomimetic system to quantitatively investigate the role of Notch signaling in regulating early angiogenic sprouting and vasculature formation of ECs in a 3D extracellular matrix. Morphological features of angiogenesis including invasion distance, invasion area, and tip cell number were quantified and compared under pharmacological perturbations of Notch signaling. In addition, influences of Notch signaling on EC proliferation in angiogenic vasculatures and directional invasion of tip cells were also investigated. Moreover, leveraging a novel nanobiosensor system, mRNA expression of Dll4, a Notch ligand, was monitored in invading tip cells using live cell imaging during the dynamic angiogenic process. Our data showed that inhibition of Notch signaling resulted in hyper-sprouting endothelial structures, while activation of Notch signaling led to opposite effects. Our results also supported the role of Notch signaling in regulating EC proliferation and dynamic invasion of tip cells during angiogenesis.

Introduction

Angiogenesis is the development of neo-blood vessels from pre-existing vascular networks, which plays a prominent role in both normal physiological processes (*e.g.*, embryonic development and wound healing) and cancer metastasis.[1–4] Angiogenesis is a highly orchestrated process, in which endothelial cells (ECs) migrate collectively, make new connections, and remodel nascent vascular structures to form functional blood vessels.[5] According to recent studies, tip cells at the head of growing angiogenic sprouts, also called leader cells, are actively involved in probing and sensing surrounding environmental cues and providing guidance to stalk cells which follow tip cells and contribute to the establishment of cell–cell junctions and vessel lumens.[6] Angiogenesis is a dynamic process, with tip cells and stalk cells constantly rearranging their relative positions. The balance and dynamics of tip cells and stalk cells during angiogenic sprouting and vasculature formation are commonly believed to depend on Delta-Notch signaling.[7,8]

Notch signaling is an evolutionarily conserved, intercellular, and contact-dependent signaling mechanism that plays a fundamental role in regulating cell fate during development and tissue homeostasis.[5,9–12] Multiple ligands are involved in Notch signaling, among which the most notable is Dll4 (Delta-like ligand 4).[9,11,13–15] A high level of Dll4 in tip cells of angiogenic sprouts activates Notch signaling in follower stalk cells to inhibit their transformation into new tip cells.[6,7,10,16,17] Previous studies have shown that inhibition of Dll4 results in a broad-spectrum antitumor activity.[9,18,19] For instance, deletion of a single allele of Dll4 inhibits tumor growth in a variety of tumor models.[20–22] However, there are also studies suggesting that Notch signaling functions as a negative regulator of tumor angiogenesis, as inhibition of Notch signaling results in hyper-angiogenic sprouting.[9,18–22] Nonetheless, the most commonly accepted theory for Notch

[a] *Department of Mechanical Engineering, University of Michigan, Ann Arbor, MI 48109, USA. E-mail: jpfu@umich.edu, allenliu@umich.edu*
[b] *Department of Precision Instrument, Tsinghua University, Beijing, 100084, P.R. China*
[c] *School of Engineering and Applied Science, University of Pennsylvania, Philadelphia, PA 19104, USA*
[d] *Department of Bioengineering, Northeastern University, Boston, MA 02115, USA*
[e] *Department of Biomedical Engineering, University of Michigan, Ann Arbor, MI 48109, USA*
[f] *Cellular and Molecular Biology Program, University of Michigan, Ann Arbor, MI 48109, USA*
[g] *Biophysics Program, University of Michigan, Ann Arbor, MI 48109, USA*
[h] *Department of Cell and Developmental Biology, University of Michigan Medical School, Ann Arbor, MI 48109, USA*

† Electronic supplementary information (ESI) available. See DOI: 10.1039/c7lc00186j

‡ Yi Zheng and Shue Wang contributed equally to this work.

signaling in tumor angiogenesis is that inhibition of Notch signaling through down-regulation of Dll4 leads to overgrowth of tumor vasculatures, even though such increased vascularity is non-productive.[9,13,21,23–25] Given its importance in tumor angiogenesis and progression, a better understanding of Notch signaling in a suitable angiogenesis model will provide new insights for targeting tumors that are resistant to anti-angiogenesis therapy.[9,26,27]

Existing investigations of the regulatory role of Notch signaling in angiogenesis primarily rely on animal models, especially mouse retina.[10,12,16,17,28,29] In contrast to humans, mouse (and other rodent) pups have an immature retinal vasculature and persistent hyaloid vessels at birth, rendering them an ideal model for studying physiological angiogenic processes.[30–32] However, even though animal models can provide physiologically relevant environments, they are not ideal for modeling human diseases, due to critical genetic, molecular, immunologic, and cellular differences between species.[33] Moreover, uncontrolled laboratory environments, difficulties in isolating single parameters, and low reproducibility of parametric studies are all intrinsic disadvantages associated with animal models. Finally, dynamic high-resolution live cell imaging is also challenging with animal tissues.

Herein, we demonstrated, for the first time, the usage of a microengineered three-dimensional (3D) biomimetic angiogenesis device to investigate the role of Notch signaling in regulating angiogenic sprouting and vasculature formation of ECs in a 3D extracellular matrix. The unique compartmentalized design of the biomimetic angiogenesis device provided physiologically relevant biomimicry for recapitulating the dynamic angiogenic sprouting process. Morphological features of angiogenesis including endothelial invasion distance and area, tip cell number, and the proliferation pattern of newly generated vasculatures were investigated and compared under different pharmacological perturbations of Notch signaling. Enabled by the 3D biomimetic angiogenesis device, the influence of Notch signaling on directional invasion of ECs during angiogenic sprouting was also examined. Importantly, a gold nanorod–locked nucleic acid (GNR–LNA) nanobiosensor was utilized in conjunction with the 3D biomimetic angiogenesis device to investigate Dll4 mRNA expression in invading tip cells at the head of angiogenic sprouts using live cell imaging. Together, our results confirmed the important role of Notch signaling in regulating morphogenesis, proliferation, and directional invasion of ECs during angiogenesis. Our data provide convincing evidence supporting the utility of the 3D biomimetic angiogenesis device for advancing the understanding of molecular and cellular mechanisms underlying angiogenesis in a 3D biomimetic and physiologically relevant environment.

Results and discussion

Design of the biomimetic angiogenesis device and mechanism of the GNR–LNA nanobiosensor

To examine the involvement of Notch signaling in angiogenesis, herein we adapted a compartmentalized microscale device, previously utilized by our group and others,[34–38] to provide an efficient biomimetic means to promote and visualize early angiogenic processes. As shown in Fig. 1A, this biomimetic angiogenesis device consisted of two parallel side channels (100 μm in height and 1000 μm in width; designated as the endothelial channel and the fibroblast channel), separated by a central channel defined by trapezoid-shaped supporting posts designed for confining fibrin gel by surface tension prior to gelation. The fibrin gel in the central channel served as a scaffold to promote angiogenic sprouting of ECs, while allowing convenient microscopic imaging to examine the morphological features of angiogenesis and Notch signaling. Human bone marrow fibroblasts (HS5) suspended in fibrin gel were carefully placed in the two reservoirs of the fibroblast channel without blocking the channel. The same fibrin gel was injected into the central gel channel. Upon fibrin gel polymerization, ECs were loaded into the endothelial channel and allowed to adhere to the gel interface in the endothelial channel by tilting the device by 90°. For pharmacological perturbations of Notch signaling, chemicals were added to culture medium and introduced into the angiogenesis device. The angiogenesis device was continuously imaged for 48 h to examine the morphological features of angiogenesis including endothelial invasion distance, invasion area, and tip cell number (ESI† Fig. S1).

A GNR–LNA nanobiosensor was utilized to examine Notch signaling during the dynamic angiogenic process in the angiogenesis device. The GNR–LNA nanobiosensor is a complex of a gold nanorod and locked nucleic acid (LNA) probe, a 20-base pair single-stranded alternating DNA/LNA oligonucleotide sequence labeled with a fluorophore (6-FAM (fluorescein)) (Fig. 1B). The LNA probe sequence is complementary to target the Dll4 mRNA sequence. Design and characterization of such GNR–LNA nanobiosensors have been reported previously.[39,40] Briefly, the LNA probe will bind to the GNR spontaneously to form the GNR–LNA complex. Due to their close physical proximity, the fluorophore of the LNA probe is quenched by the GNR. After internalization by cells and in the presence of target mRNA molecules in the cytoplasm, the LNA probe disassociates from the GNR before binding target mRNA molecules while reacquiring a fluorescence signal (Fig. 1B). Thus, the fluorescence intensity of individual cells containing the GNR–LNA nanobiosensor can serve as a quantitative measure of the amount of target mRNA molecules inside individual single cells.[41,42] In this study, ECs were cultured with the GNR–LNA probe prior to cell seeding into the angiogenesis device. Internalized GNR–LNA probes in the ECs through endocytosis were clearly evident in the dark-field image in Fig. 1C.

Involvement of Notch signaling in angiogenesis

Using the 3D biomimetic angiogenesis device, we first examined the involvement of Notch signaling in regulating angiogenic sprouting of ECs using two well-characterized pharmacological drugs, DAPT and Jagged1 peptide (Fig. 1D).[11,14,42]

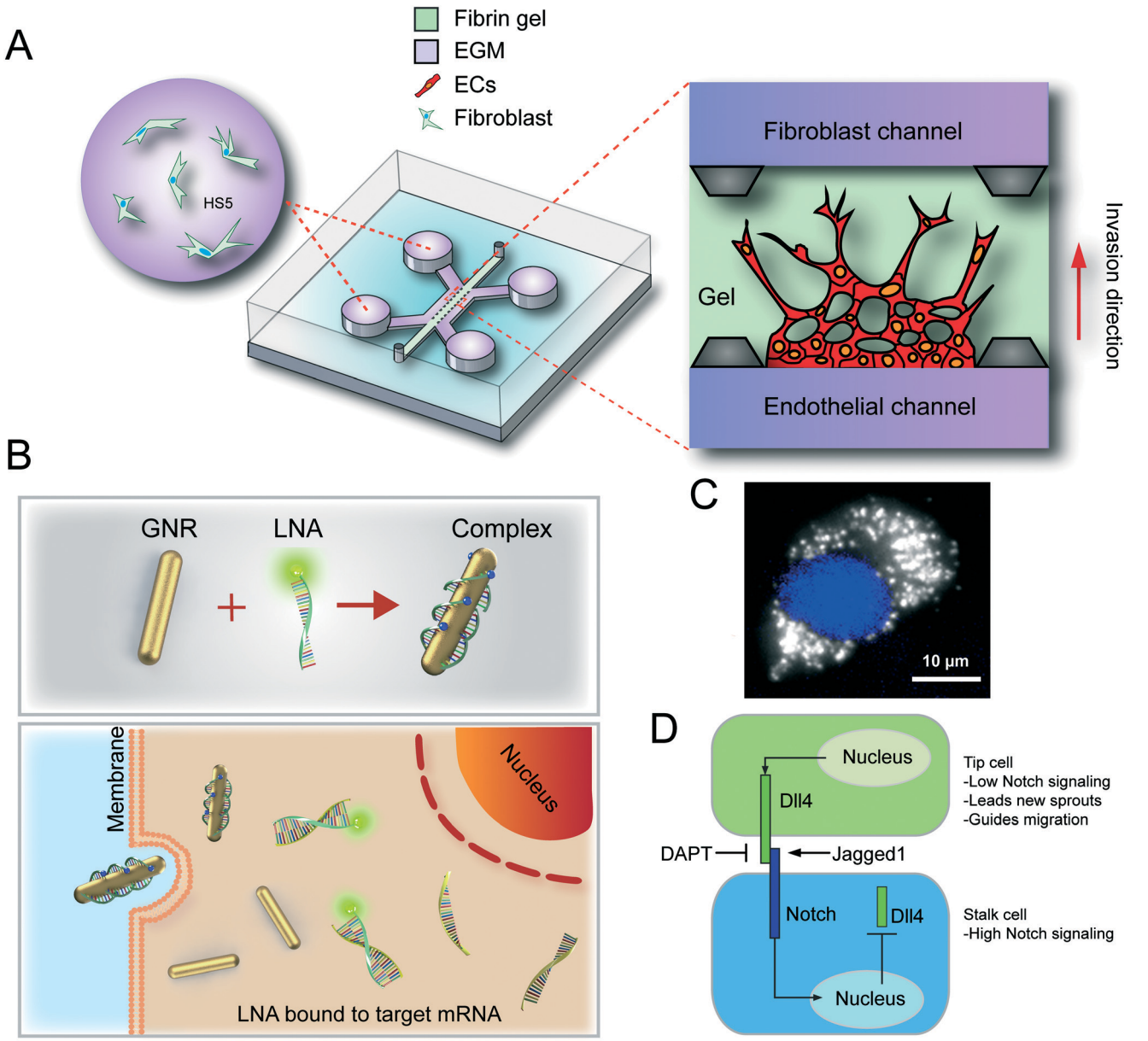

Fig. 1 A 3D microengineered biomimetic angiogenesis device and the gold nanorod–locked nucleic acid (GNR–LNA) nanobiosensor for investigation of Notch signaling in angiogenesis. (A) Schematic of the 3D angiogenesis device and cell seeding configuration. Two side channels (designated as the endothelial channel and the fibroblast channel) were separated by the central (gel) channel filled with fibrin gel. Endothelial cells (ECs) were loaded into the endothelial channel and allowed to adhere onto the gel interface, whereas human bone marrow fibroblasts (HS5) suspended in fibrin gel were placed in the two reservoirs of the fibroblast channel. Paracrine interaction between HS5 and ECs led to invasion of ECs into the central gel region to form neovessels. (B) Biosensing mechanism of the GNR–LNA nanobiosensors. Binding of the LNA probe, a 20-base nucleic acid molecule labeled with a fluorophore (6-FAM (fluorescein)) at the 5′ end, to GNR quenches the fluorophore. After internalization by ECs *via* endocytosis, LNA probes bind targeted mRNA in the cytoplasm and reacquire fluorescence. The fluorescence intensity thus serves as an indicator of the expression level of target mRNA. (C) Dark-field image showing an EC with internalized GNR (bright spots in the image). DAPI staining (blue) labels the nucleus. (D) Notch signaling between a tip cell and a stalk cell.

DAPT is a γ-secretase inhibitor that blocks Notch endoproteolysis and thus serves indirectly as a Notch inhibitor. Jagged1 peptide (hereafter referred to as Jagged1) can activate Notch signaling by inhibiting the function of endogenous Jagged1, a Notch ligand that has weak signaling capacity but competes with Dll4.

HS5 cells cultured in the fibroblast channel reservoirs could effectively induce angiogenesis of ECs into the fibrin gel by establishing growth factor gradients in the gel (ESI† Fig. S1 and 2A).[38] 48 h after initial cell seeding, we observed prominent directional migration and invasion of ECs from the endothelial channel into the fibrin gel toward the fibroblast channel forming neo-blood vessel networks (ESI† Fig. S1, S2 and 2A). Pharmacological treatments with DAPT and Jagged1 effectively induced morphological changes of invading tip cells and blood vessel networks. Specifically, both

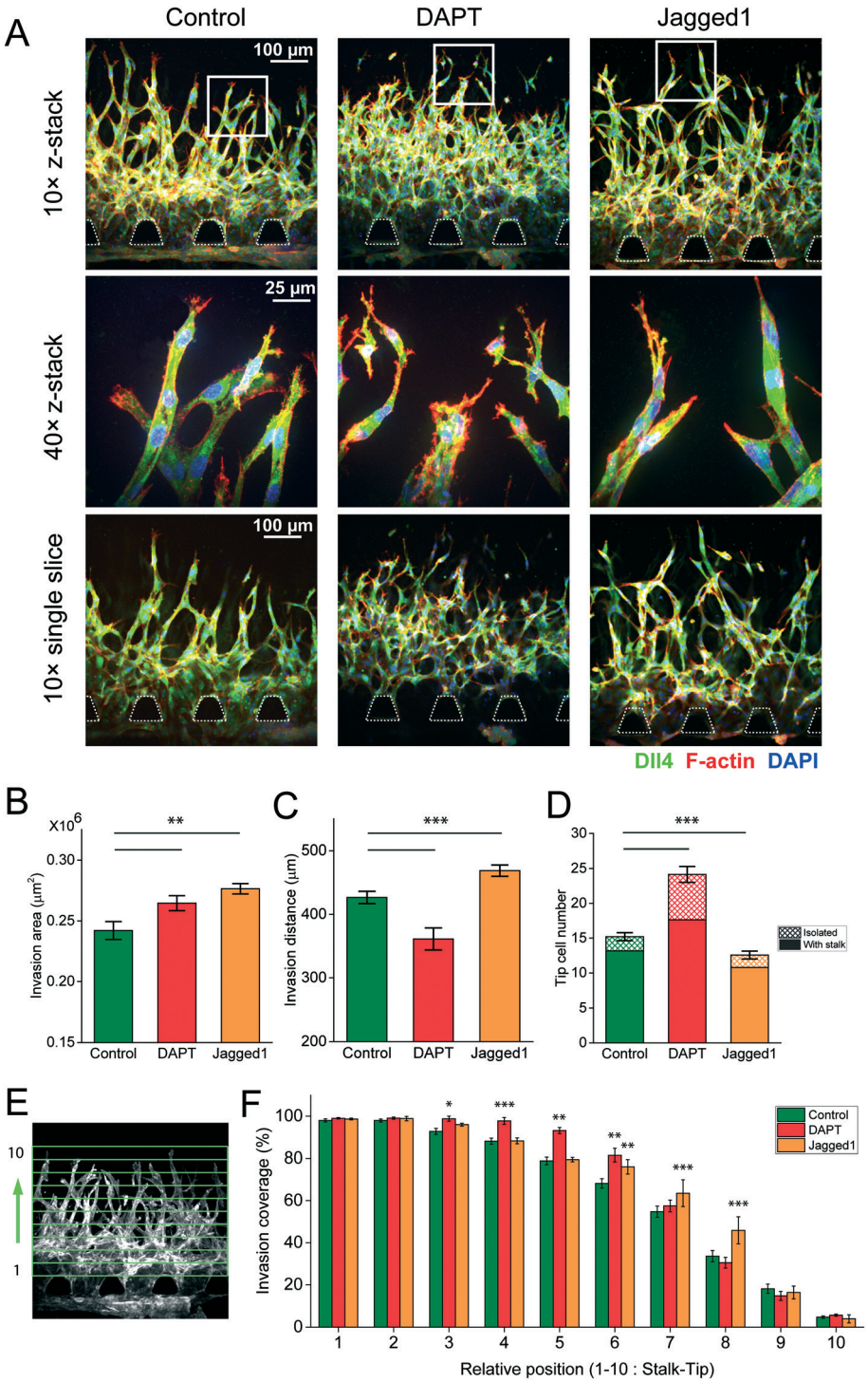

Fig. 2 Involvement of Notch signaling in regulating angiogenic morphogenesis. (A) Representative confocal images in *z*-projection showing angiogenic morphogenesis of ECs treated without (control) or with 20 μM DAPT or 20 μM Jagged1 as indicated. Images were acquired 48 h after initial cell seeding. Samples were stained for Dll4 (green), F-actin (red; by phalloidin), and nucleus (blue; by DAPI), respectively. Dashed trapezoids highlight PDMS supporting structures at the fibrin gel interface within the endothelial channel. The white rectangles in the top images mark the areas recorded using 40× objectives to show tip cell morphologies (middle). Single confocal image slices (bottom) show branching of neo-blood vessel networks. (B–D) Bar plots of invasion area (B), invasion distance (C), and tip cell number (isolated: crosshatch, with stalks: solid; D) under different conditions as indicated. (E) Representative confocal image slices showing 10 sub-regions with equal areas between supporting posts and leading tip cells. (F) Quantification of angiogenic invasion area coverage (%) in the 10 sub-regions between supporting posts and leading tip cells under different conditions as indicated. Error bars, S.E.M., with n = 10–15 fields of view from >4 devices. p-Values were calculated using a two-sample t-test with respect to control. *, $p < 0.05$; **, $p < 0.01$; ***, $p < 0.005$.

DAPT and Jagged1 treatments led to increased branching in the vascular network compared with the untreated control. In addition, compared with the untreated control, under DAPT treatment, tip cells located at the invasion front of angiogenic sprouting possessed more tiny sprouts, particularly for the furthest tip cells. For ECs treated with Jagged1, the cell membrane of tip cells appeared much smoother, consistent with the theory that Notch signaling serves as a negative regulator to control the potency of ECs sprouting from an existing vascular network.[5,9–12]

We further quantified the effects of DAPT and Jagged1 treatments on the invasion area, invasion distance, and tip cell number during angiogenic sprouting and blood vessel formation of ECs in the angiogenesis device. Both DAPT and Jagged1 treatments led to an overall increase of invasion area into the fibrin gel during angiogenesis (Fig. 2B). Inhibition of Notch signaling by DAPT led to decreased invasion distance but potently increased tip cell number (including both isolated tip cells and tip cells with stalks) during angiogenic sprouting (Fig. 2C and D). These observations are in good agreement with *in vivo* experiments reported in the literature,[10,17,28,43] in which inhibition of Notch signaling has resulted in greater tip cell numbers and larger angiogenic invasion area. In contrast, up-regulation of Notch signaling by Jagged1 resulted in increased EC invasion but decreased tip cell numbers (including both isolated tip cells and tip cells with stalks; Fig. 2C and D), also in agreement with *in vivo* studies.[5,9–12]

Even though both DAPT and Jagged1 treatments led to an overall increase of invasion area of angiogenic sprouting, spatial features of angiogenic sprouting were distinct between DAPT- and Jagged1-treated samples. To quantify such spatial angiogenesis features, we divided the rectangular area between trapezoid-shaped supporting posts (where ECs were initially seeded) and the furthest leading tip cell into ten sub-regions of equal areas (labeled from 1–10; Fig. 2E). Invasion coverage percentage, defined as the ratio of projected area covered by ECs and the area of each sub-region, was calculated for each sub-region (ESI† Fig. S3). As shown in Fig. 2F, vascular network formation under Jagged1 treatment showed higher invasion coverage percentage, compared with the untreated control, in sub-regions close to the invasion front, whereas DAPT treatment led to higher invasion coverage in areas closer to the supporting posts where ECs were initially seeded. These morphogenetic distinctions could possibly be resulted from altered proliferation or invasion potency of ECs under different pharmacological perturbations of Notch signaling. These possibilities were further investigated in the following sections. Together, our data supported that DAPT treatment led to EC hypersprouting, resulting in a "nonfunctional vasculature" exhibiting limited resemblance to normal vascular networks.[6,8,15,24,27] Even though Jagged1 treatment led to increased branching in the vessel network, such vascular architecture possessed a greater similarity to the untreated control.

Notch signaling regulates EC proliferation during angiogenesis

Based on the distinct morphological features of neo-blood vessel formation during angiogenesis observed in Fig. 2, we hypothesized that, in addition to invading tip cell behaviors, proliferation and remodeling of follower stalk cells might also be important for establishing such distinct morphological features of vascular networks under different conditions. To examine this possibility, Click-iT EdU assays were conducted to identify EdU-positive, proliferating ECs in the fibrin hydrogel (Fig. 3A; see Materials and methods). As shown in Fig. 3B and C, the number of EdU-positive nuclei in the fibrin gel was significantly greater under both DAPT and Jagged1 treatments compared with the untreated control. However, the percentages of EdU-positive nuclei relative to the total cell number (as labeled by DAPI) under DAPT and Jagged1 treatments were comparable with that for the untreated control (Fig. 3B), suggesting that DAPT and Jagged1 treatments did not alter the proliferative behavior of ECs in the fibrin gel, but had caused more ECs to invade into the gel. This contention was further supported by standard cell proliferation and toxicity assays conducted using transwells (see Materials and methods), revealing no significant differences in cell proliferation or toxicity between different monoculture or co-culture conditions treated without or with DAPT or Jagged1 (ESI† Fig. S4).

We further examined spatial patterns of EC proliferation in angiogenic vasculatures in the fibrin hydrogel, by dividing the rectangular area between supporting posts (where ECs were initially seeded) and the furthest leading tip cell into ten equal sub-regions. Under all experimental conditions, the highest percentages of EdU-positive cell nuclei were in the middle portion of the vessel network, while both tip cells and ECs located close to supporting posts showed the lowest percentages of EdU-positive nuclei (Fig. 3D). Compared with the control, DAPT treatment resulted in lower percentages of proliferating EdU-positive ECs near the invasion front and greater cell proliferation for the rest of the vasculature regions in the fibrin hydrogel (Fig. 3D). In contrast, Jagged1 treatment led to significantly greater EC proliferation at the invasion front but less proliferation for the rest of the vasculature regions in the fibrin hydrogel compared with the untreated control (Fig. 3D). These distinct spatial patterns of EC proliferation under different conditions could partially explain the greater invasion coverage in the middle portion of the vascular network under DAPT treatment and the higher invasion coverage at the invasion front under Jagged1 treatment when compared with the untreated control. In conclusion, manipulation of Notch signaling using pharmacological drugs didn't affect the overall proliferation rate of ECs. Under DAPT treatment, a higher percentage of ECs were "trapped" in the vicinity around the supporting posts where the cells were initially seeded, likely due to compromised migratory potency of ECs, the evidence of which is presented in the following section.

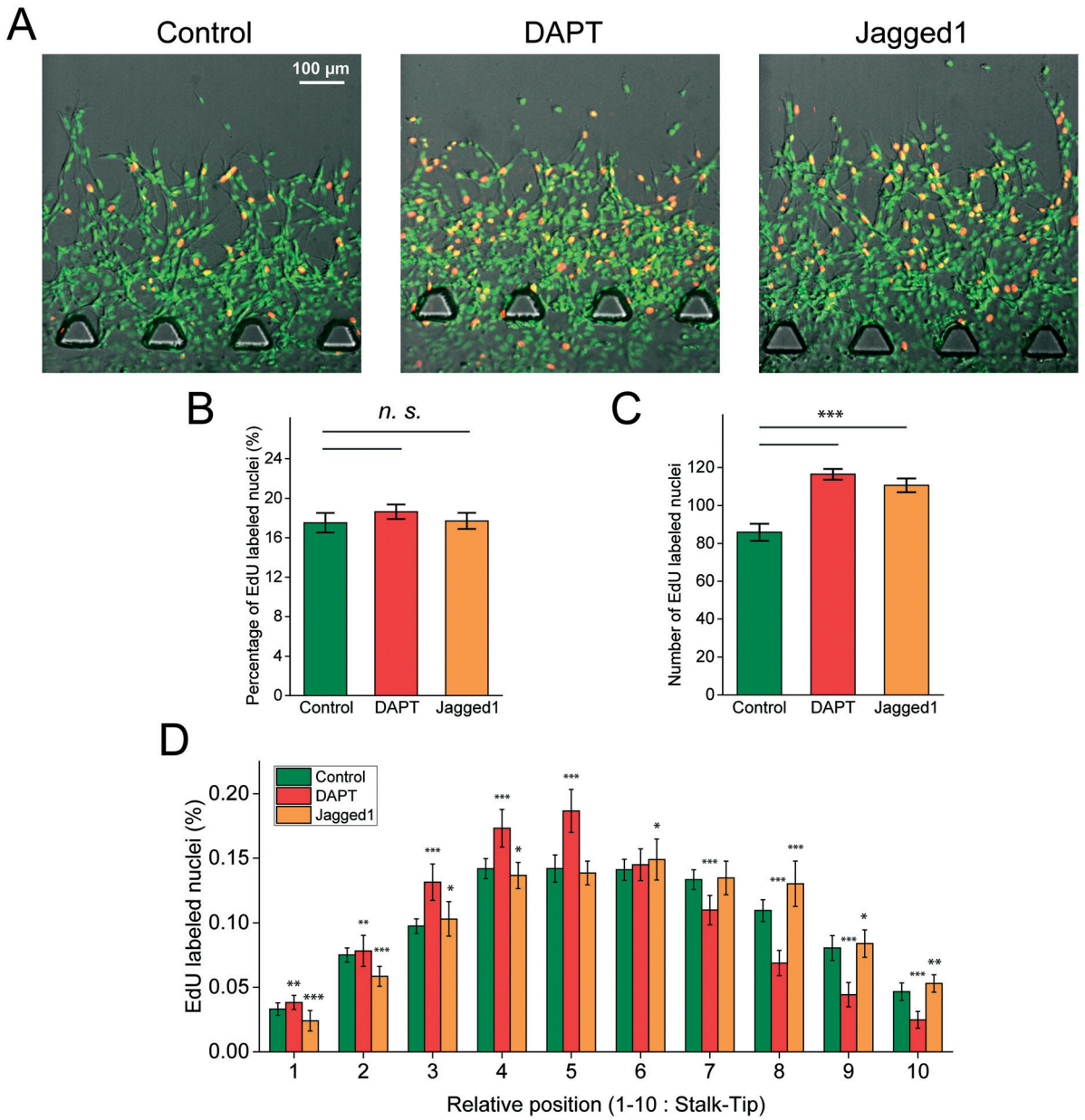

Fig. 3 Involvement of Notch signaling in regulation of proliferation of ECs during angiogenesis. (A) Fluorescence images showing proliferation of invading ECs in the fibrin gel. Images were taken 21 h after initial cell seeding. Cell nuclei with newly synthesized DNA within the last 3 h were labeled in red using the Click-iT EdU Imaging Kit (Invitrogen), while all cell nuclei were labeled in green. Bright-field images were superimposed to outline angiogenic sprouts. (B & C) Percentage (B) and number (C) of EdU-labeled nuclei in the angiogenic network per field of view. (D) Bar plot showing the percentage of EdU-labeled nuclei in the 10 sub-regions between supporting posts and leading tip cells under different conditions as indicated. Error bars, S.E.M., with n = 10–15 fields of view from >4 devices. p-Values were calculated using a two-sample t-test with respect to control. *, $p < 0.05$; **, $p < 0.01$; ***, $p < 0.005$.

Notch signaling in regulation of directional invasion of ECs

Our data so far suggested that the role of Notch signaling in regulating angiogenic morphogenesis was likely through its effect on mediating tip cell behaviors. Thus, we further performed live cell imaging to track migratory behaviors of individual tip cells during angiogenesis using ECs expressing red fluorescent protein (RFP) (Fig. 4A). Tip cells were continuously monitored for 48 h after initial cell seeding (Fig. 4A; videos supplemented as ESI† GIF 1, 2 and 3). In the angiogenesis device, tip cells preferentially migrated in the fibrin gel along growth factor gradients established toward the fibroblast channel with a relatively narrow range of cell migration orientation angles between ±25°.

To further evaluate the directionality of tip cell invasion, distributions of the migration orientation angle of tip cells were plotted in polar histograms (Fig. 4B). Perturbations of Notch signaling using DAPT and Jagged1 induced significant changes of tip cell migratory behaviors. Specifically,

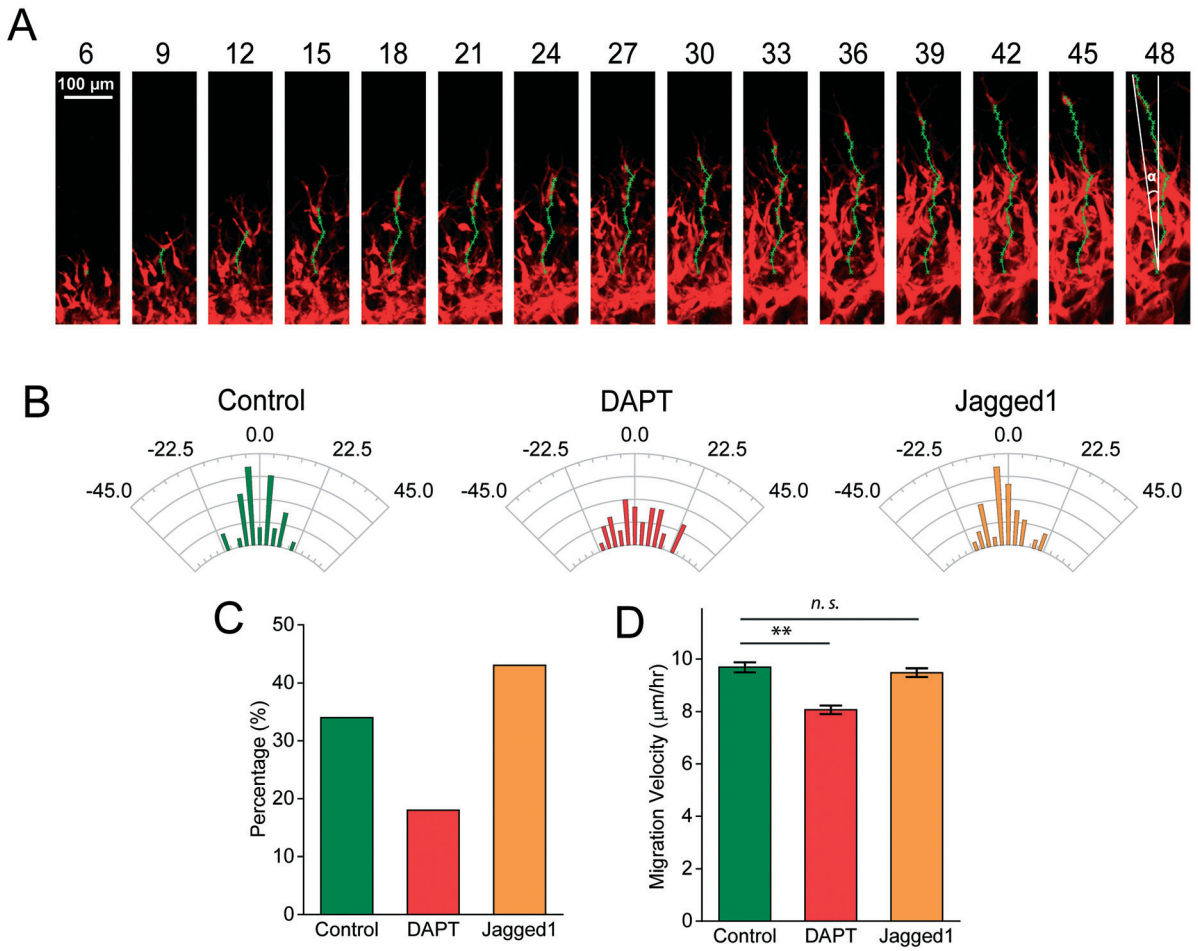

Fig. 4 Notch signaling regulates directional invasion of ECs during angiogenesis. (A) Live-cell confocal images showing dynamic directional EC invasion in the fibrin hydrogel under the control conditions. The orientation angle α of tip cell invasion was calculated using coordinates of the starting and end points of an individual cell invasion trajectory 48 h after initial cell seeding as shown in the last image. (B) Polar histograms showing distribution of the orientation angle of tip cell invasion trajectory without (control) or with DAPT and Jagged1 treatments as indicated. Each bar in the histograms represents the percentage of orientation angle across the entire population. (C & D) Bar plots showing the percentage of tip cells with the orientation angle α within ±4° (C) and migration velocity of tip cells (D) under different conditions as indicated. Error bars, S.E.M., with n = 40–50 cells from two devices. p-Values were calculated using a two-sample t-test with respect to control. *, $p < 0.05$; **, $p < 0.01$; ***, $p < 0.005$.

inhibition of Notch signaling by DAPT resulted in a decreased fraction of tip cells migrating along growth factor gradients toward the fibroblast channel, whereas activation of Notch by Jagged1 increased this fraction. This observation is also reflected in Fig. 4C where percentages of invading tip cells with migration orientation angles falling between ±4° were compared between different conditions (control: 34%; DAPT: 18%; Jagged1: 44%). Notably, we also observed decreased migration velocity for DAPT-treated ECs, but not for Jagged1-treated cells (Fig. 4D), suggesting that inhibition of Notch signaling negatively impacted both tip cell invasion directionality and speed.

Notch signaling in regulation of Dll4 mRNA expression

We further utilized the GNR–LNA nanobiosensor in conjunction with the 3D angiogenesis device to examine Dll4 mRNA expression in invading tip cells at the head of angiogenic sprouts. The GNR–LNA probe was designed to target specifically Dll4 mRNA, and its specificity was validated using 2D culture assays before implementing it for 3D angiogenesis experiments (ESI† Fig. S5). A random probe was also included in this work as a negative control (ESI† Fig. S6). ECs were incubated with GNR–LNA probes for 4 h to allow cellular uptake before seeding cells at the fibrin gel interface. Tip cells treated without (control) or with DAPT and Jagged1 were continuously monitored in the 3D angiogenesis device for 18 h after initial cell seeding (Fig. 5A and ESI† Fig. S7). Live imaging of the 3D angiogenesis device to monitor single-cell Dll4 mRNA expression was limited to 18 h due to photobleaching. As shown in Fig. 5B and C, compared with the untreated control or cells treated with Jagged1, tip cells treated with DAPT consistently exhibited higher fluorescence intensity, suggesting greater Dll4 mRNA expression in DAPT-treated tip

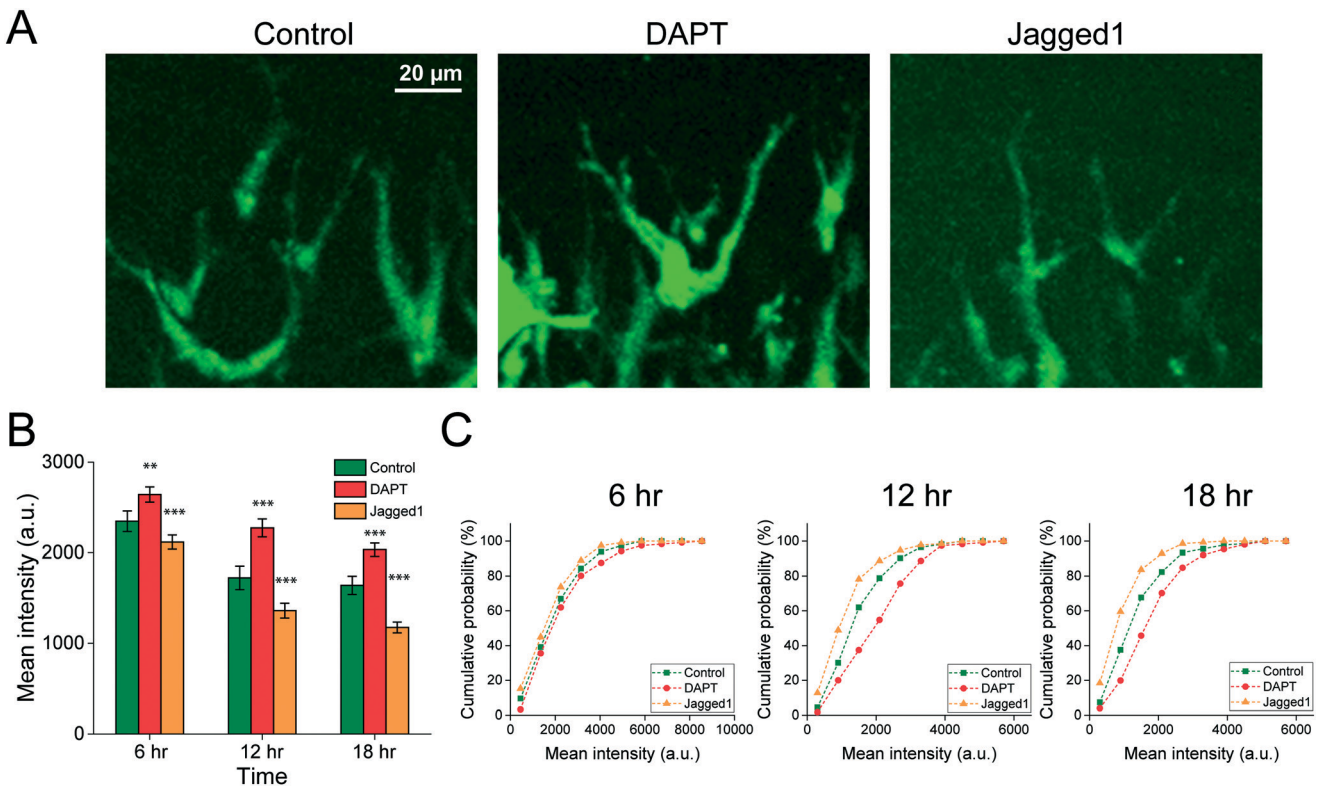

Fig. 5 Dll4 mRNA expression in tip cells during angiogenesis. (A) Confocal images showing fluorescence signals from GNR–LNA nanobiosensors for detection of Dll4 mRNA in invading tip cells under different conditions as indicated. Images were recorded 12 h after initial cell seeding. (B) Mean fluorescence intensity of invading tip cells at different time points after initial cell seeding under different conditions as indicated. (C) Cumulative probability of tip cell fluorescence intensity (see Materials and methods) at different time points after initial cell seeding under different conditions as indicated. Error bars, S.E.M., with n = 130–150 cells from 3 devices. p-Values were calculated using a two-sample t-test with respect to control. *, $p < 0.05$; **, $p < 0.01$; ***, $p < 0.005$.

cells. In contrast, Jagged1 treatment led to significantly decreased Dll4 mRNA expression in tip cells. Differences in fluorescence intensity and thus Dll4 mRNA expression in tip cells between different conditions (DAPT *vs.* control and Jagged1 *vs.* control) became greater over time. These observations were further confirmed using EC networks formed on 2D Matrigel substrates (ESI† Fig. S5).

Conclusion

The Notch signaling pathway is an evolutionarily conserved intercellular pathway that is important in regulating cell fate patterning during normal development and tissue homeostasis.[44] There are four Notch receptors, including Notch1, Notch2, Notch3 and Notch4, and five Notch transmembrane ligands, including Jagged1, Jagged2, Delta-like 1 (Dll1), Dll3 and Dll4.[5] Notch signaling mediated through Dll4 has been particularly suggested to negatively regulate tip cell formation during angiogenesis and control leader cell formation during collective epithelial cell migration.[28,45,46] In this study, we demonstrated, for the first time, the usage of a microengineered 3D biomimetic device to examine the role of Notch signaling in regulating angiogenic sprouting and vasculature formation. The administration of γ-secretase inhibitor DAPT, which inhibits Notch signaling through blocking Notch cleavage and signaling, to ECs in our biomimetic device resulted in an abnormal angiogenic network, including hyper-sprouting endothelial structures, and increased tip cell number and invasion area, consistent with previous *in vivo* experiments.[10,17,28,43] In contrast, activation of Notch signaling through Jagged1 treatment showed the opposite effects, including increased invasion distance but decreased tip cell number, also in agreement with *in vivo* studies.[5,9–12] Moreover, enabled by the 3D biomimetic angiogenesis device, the influences of Notch signaling on EC proliferation in newly generated neo-blood vessel networks and directional migration of invading tip cells were also investigated, with findings supporting the potent role of Notch signaling in regulating angiogenic dynamics of ECs. By using the GNR–LNA nanobiosensor for Dll4 mRNA detection, we further examined Dll4 mRNA expression in invading tip cells at the head of angiogenic sprouts. Our results suggested that DAPT and Jagged1 treatments perturbed Dll4 mRNA expression in tip cells during angiogenic sprouting, which could explain the different angiogenic sprouting phenotypes observed under DAPT and Jagged1 treatments. Together, the capability of the 3D biomimetic angiogenesis device to recapitulate *in vivo* 3D microenvironments,

combined with the application of live-cell nanobiosensors, enabled us to study in detail the role of Notch signaling in regulating angiogenesis. The 3D biomimetic angiogenesis device offers excellent assay repeatability and allows for live cell imaging at a high spatiotemporal resolution, which will provide an attractive alternative approach to existing animal models for studying angiogenesis.

Materials and methods

Device fabrication

The 3D microengineered biomimetic angiogenesis device consisted of a polydimethylsiloxane (PDMS) microchannel layer and a bottom coverslip. The PDMS microchannel layer was fabricated using soft lithography. PDMS was mixed at a 1 : 10 curing agent-to-elastomer base ratio and casted onto a positive mold made of SU-8 patterned using standard lithography, then cured at 120 °C for 20 min. Four loading reservoirs and two gel loading inlets were punched into the PDMS layer by 8 mm and 1.2 mm Harris Uni-Core punch tools (Ted Pella), respectively. The PDMS microchannel layer and the coverslip were cleaned with ethanol and treated with oxygen plasma for 80 s before bonding them together. The 3D angiogenesis device was baked at 80 °C for 2 h to restore surface hydrophobicity before further sterilization by exposing to UV light for 25 min.

Cell culture

Two cell lines were used in this work: human umbilical vein endothelial cells (HUVECs) and bone marrow stromal fibroblasts (HS5). HUVECs and HS5 were acquired from Lonza and ATCC, respectively. HUVECs were maintained in endothelial cell growth medium-2 (EGM; Lonza) and harvested using 0.05% trypsin–EDTA (Lonza) when cells reached 90% confluency. Passages 2–5 were used for HUVECs. HS5 cells were cultured in DMEM basal medium supplemented with 10% FBS and 0.5% penicillin–streptomycin. All cells were cultured under 5% CO_2 at 37 °C, and culture medium was exchanged every 2 days.

Cell seeding

Fibrinogen (Sigma) was dissolved in PBS at a concentration of 2.5 mg mL^{-1} before being supplemented with aprotinin (0.15 U mL^{-1}, Sigma). HS5 cells were then suspended in the fibrinogen solution at a concentration of 2×10^6 cells per mL before mixing with thrombin (0.5 U mL^{-1}) and loaded into the two reservoirs of the fibroblast channel without blocking the channel.[35,47] The same fibrin gel was prepared and injected into the middle gel channel of the 3D angiogenesis device. The 3D angiogenesis device was then incubated at 37 °C for 15 min to allow complete gelation of the fibrin gel. EGM solution (300 μL) was then added to the 4 loading reservoirs of the endothelial and fibroblast channels before filling the channels with EGM solution by gently applying vacuum. The 3D angiogenesis device was incubated for another 24 h to eliminate bubbles trapped inside the device. 20 μL HUVEC solution with a cell concentration of 5×10^6 cells per mL was introduced into the endothelial channel. The 3D angiogenesis device was then tilted by 90° and incubated for 15 min at 37 °C to allow HUVECs to adhere to the fibrin gel interface.

To examine the involvement of Notch signaling in regulating angiogenic sprouts, HUVECs were cultured with EGM supplemented with 20 μM γ-secretase inhibitor DAPT (Sigma) and 20 μM Jagged1 peptide (188-204, AnaSpec). After cell seeding, the 3D angiogenesis device was incubated at 37 °C with 5% CO_2 and monitored for 2 days, with culture medium exchanged daily.

Immunofluorescence staining

The vascular network in the 3D angiogenesis device was washed 3 times with PBS, 10 min each time. Cells were then fixed with 4% paraformaldehyde solution (PFA) for 10 min before being permeabilized and blocked with the Perm/Block solution PBST (PBS + 0.5% Triton + 1% BSA) for 1 h. After washing with PBS 3 times to remove PBST, the cells were incubated with primary Dll4 antibodies diluted in PBST (1 : 200, R&D) at 4 °C overnight. After incubation, the cells were washed 3 times with PBST, 15 min each time. The cells were then incubated with Dll4 secondary antibodies (1 : 500, Abcam), phalloidin (1 : 30), and DAPI (1 : 2000) for 2 h at room temperature (all chemicals diluted in PBST). The cells were then washed 3 times with PBST, 15 min each time, before fluorescence imaging and analysis.

Imaging and analysis

Immunofluorescence images of vascular networks in the 3D angiogenesis device were recorded using an Olympus DSU-IX81 spinning disc confocal microscope equipped with an EMCCD camera (iXon X3, Andor). *Z*-stack images were acquired with a slice thickness of 1 μm. Time-lapse images of angiogenesis were acquired during a time period of 48 h with an interval of 30 min after initial cell seeding. Cells were kept at 37 °C using a Tokai Hit incubator chamber placed on top of the microscope stage. Migration trajectories of individual invading tip cells were tracked manually using the MTrackJ plugin of ImageJ. The orientation angle of tip cell invasion was calculated using coordinates of the starting and end points of an individual cell invasion trajectory. Fluorescence images of EC angiogenesis with internalized GNR–LNA probes were also acquired using confocal microscopy at 6, 12 and 18 h after cell seeding and analyzed with ImageJ to determine the fluorescence intensity of LNA probes.

Probe design

LNA probes for Dll4 mRNA have 20 base pair nucleotides (+AA+GG+GC+AG+TT+GG+AG+AG+GG+TT) designed for capturing Dll4 mRNA with a nucleotide sequence complementary to the probe. For mRNA detection, a fluorophore (6-FAM

(fluorescein)) was attached to the 5′ end of the LNA probe. The specificity of the Dll4 mRNA probe sequence was characterized using the NCBI Basic Local Alignment Search Tool (BLAST) database. A random probe (+AC+GC+GA+CA+AG+CG +CA+CC+GA+TA) was designed as negative control. All LNA probes were synthesized by Integrated DNA Technologies.

GNR–LNA probe preparation

GNRs with a diameter of 10 nm and a length of 67 nm were acquired from Nanopartz. The GNRs were coated with 11-mercaptoundecyltrimethylammonium bromide (MUTAB) for enhancing cellular uptake and their ability to bind LNA probes. LNA probes were diluted in Tris–EDTA buffer at a concentration of 10 mM before incubation with GNRs at 37 °C for 30 min. The GNR–LNA probes were then incubated with cells for endocytic uptake.

GNR–LNA probe assay

HUVECs were seeded in a T25 cell culture flask with a seeding density of 5×10^4 cells per mL. When the cells reached 80% confluency, GNR–LNA nanobiosensors were added into the flask and incubated with HUVECs for 4 h for endocytic uptake. After intracellular delivery of the GNR–LNA probes, the cells were washed 3 times with PBS to remove extra probes, before harvesting using 0.05% trypsin–EDTA. For 2D Matrigel assays, glass-bottom 24-well cell culture plates were treated with plasma for 1 min and coated with Matrigel (Corning). HUVECs were seeded into the Matrigel-coated wells at a seeding density of 200 cells per mm^2. Self-organized EC microvasculature networks were recorded every 3 h for 12 h using fluorescence microscopy. For microfluidic angiogenesis assays, HUVECs were seeded onto the fibrin gel interface within the endothelial channel before imaging every 6 h for 18 h using fluorescence microscopy.

The fluorescence intensity of the GNR–LNA nanobiosensors is presented in arbitrary units (a.u.). Cumulative probability (Fig. 5C) refers to the probability that the fluorescence intensity of tip cells is lower than or equal to the intensity value at the *x*-axis.

Cell viability assay

To evaluate the cytotoxicity of GNRs, DAPT, and Jagged1, the viability of ECs was characterized using a cell cytotoxicity assay (Cell Counting Kit-8 or CCK-8, Sigma) according to the manufacturer's instructions. Briefly, HUVECs were suspended in a 96-well plate with 5000 cells per well. HUVECs were incubated with GNRs, or treated with 20 μM DMSO, 20 μM DAPT, or 20 μM Jagged1 for 24 h or 48 h. The CCK-8 solution was then added to each well for 2 h. The absorbance of samples in each well was measured at 450 nm using a microplate reader (BioRad).

Transwell cell proliferation assay

The effect of stromal fibroblasts HS5 on EC proliferation was evaluated using a transwell 96-well plate (HTS transwell plate, Corning). HUVECs and HS5 were separated by a porous membrane with a 0.8 μm pore size in the transwell chamber. HUVECs were seeded at 2000 cells per well into the lower compartment of the transwell. HS5 cells were mixed with the fibrin gel before seeding into the transwell insert chamber. Culture medium was exchanged after 24 h of incubation. After 2 days of co-culture, the upper transwell chamber was removed, and the CCK-8 solution was added to the lower compartment of the transwell and incubated for an additional 1 h. The absorbance of samples was measured at 450 nm using a microplate reader every hour for 4 h at 37 °C.

In situ proliferation assay

For *in situ* proliferation measurements, Click-iT EdU Kit (Invitrogen) was used as per manufacturer's protocol. HUVECs in the 3D angiogenesis device were cultured with EGM or with EGM supplemented with either 20 μM DAPT or 20 μM Jagged1 for 21 h. Diluted EdU solution (10 μM) was then introduced into all reservoirs of the device. Before fixation, cells were incubated with EdU solution for 3 h to label newly synthesized DNA. The numbers of total nuclei (stained with Hoechst) and EdU-labeled nuclei in the confocal images were counted manually.

Quantification of invasion distance, invasion area, and tip cell number

The tip cell number was selected as a morphological indicator of vascular networks. Based on our observation, tip cell number can properly describe angiogenic morphogenic differences in the 3D biomimetic angiogenesis device, especially when isolated tip cells are prevailing. For each confocal image (*Z*-scanning images with a slice thickness of 1 μm), the number of tip cells (either trailed with a multicellular stalk or isolated) was assessed blindly by two independent observers. The vertical distance between leading tip cells and the fibrin gel interface within the endothelial channel was quantified as the invasion distance. A custom-designed MATLAB image processing program was used for quantification of invasion area and coverage percentage. Briefly, after adaptive filtering, binarization with an adaptive threshold was applied to each image. Projected area in the binarized images was measured as the invasion area. A rectangular area was placed between trapezoid-shaped supporting posts and leading tip cells to define a region of interest (ROI). The ROI was segmented into 10 sub-regions with equal areas, designated as 1–10 starting from supporting posts toward leading tip cells. For each sub-region, the coverage percentage was calculated as the ratio between the number of pixels with a binary value of 1 and the total pixels of the sub-region.

Statistical analysis

Results were analyzed using independent, two-tailed Student's *t*-test in Excel (Microsoft). $P < 0.05$ was considered statistically significant.

Acknowledgements

The authors acknowledge the financial support from the National Science Foundation (CBET 1149401 and CMMI 1536087 to J. F.; CMMI 1562043 to A. P. L.). Y. Zheng is also partially supported by the Natural Sciences and Engineering Research Council of Canada (NSERC) Postdoctoral Fellowship. The Lurie Nanofabrication Facility at the University of Michigan, a member of the National Nanotechnology Infrastructure Network (NNIN) funded by the National Science Foundation, is acknowledged for support in microfabrication. We also thank Meng-Ting Chung for his help on dark-field imaging.

References

1 A. S. Chung and N. Ferrara, Developmental and Pathological Angiogenesis, *Annu. Rev. Cell Dev. Biol.*, 2011, **27**, 563–584.
2 G. Bergers and L. E. Benjamin, Tumorigenesis and the angiogenic switch, *Nat. Rev. Cancer*, 2003, **3**, 401–410.
3 S. M. Weis and D. A. Cheresh, Tumor angiogenesis: molecular pathways and therapeutic targets, *Nat. Med.*, 2011, **17**, 1359–1370.
4 N. S. Vasudev and A. R. Reynolds, Anti-angiogenic therapy for cancer: Current progress, unresolved questions and future directions, *Angiogenesis*, 2014, **17**, 471–494.
5 R. Blanco and H. Gerhardt, VEGF and Notch in tip and stalk cell selection, *Cold Spring Harbor Perspect. Med.*, 2013, **3**, 1–19.
6 H. Serra, I. Chivite, A. Angulo-Urarte, A. Soler, J. D. Sutherland, A. Arruabarrena-Aristorena, A. Ragab, R. Lim, M. Malumbres, M. Fruttiger, M. Potente, M. Serrano, À. Fabra, F. Viñals, O. Casanovas, P. P. Pandolfi, A. Bigas, A. Carracedo, H. Gerhardt and M. Graupera, PTEN mediates Notch-dependent stalk cell arrest in angiogenesis, *Nat. Commun.*, 2015, **6**, 7935.
7 K. Bentley, C. A. Franco, A. Philippides, R. Blanco, M. Dierkes, V. Gebala, F. Stanchi, M. Jones, I. M. Aspalter, G. Cagna, S. Weström, L. Claesson-Welsh, D. Vestweber and H. Gerhardt, The role of differential VE-cadherin dynamics in cell rearrangement during angiogenesis, *Nat. Cell Biol.*, 2014, **16**, 309–321.
8 J. Bernier-Latmani, C. Cisarovsky, C. S. Demir, M. Bruand, M. Jaquet, S. Davanture, S. Ragusa, S. Siegert, O. Dormond, R. Benedito, F. Radtke, S. A. Luther and T. V. Petrova, DLL4 promotes continuous adult intestinal lacteal regeneration and dietary fat transport, *J. Clin. Invest.*, 2015, **125**, 4572–4586.
9 Z. Liu, F. Fan, A. Wang, S. Zheng and Y. Lu, Dll4-Notch signaling in regulation of tumor angiogenesis, *J. Cancer Res. Clin. Oncol.*, 2014, **140**, 525–536.
10 R. Benedito, C. Roca, I. Sörensen, S. Adams, A. Gossler, M. Fruttiger and R. H. Adams, The Notch Ligands Dll4 and Jagged1 Have Opposing Effects on Angiogenesis, *Cell*, 2009, **137**, 1124–1135.
11 N. S. Patel, J. L. Li, D. Generali, R. Poulsom, D. W. Cranston and A. L. Harris, Up-regulation of delta-like 4 ligand in human tumor vasculature and the role of basal expression in endothelial cell function, *Cancer Res.*, 2005, **65**, 8690–8697.
12 Z.-J. Liu, T. Shirakawa, Y. Li, A. Soma, M. Oka, G. P. Dotto, R. M. Fairman, O. C. Velazquez and M. Herlyn, Regulation of Notch1 and Dll4 by vascular endothelial growth factor in arterial endothelial cells: implications for modulating arteriogenesis and angiogenesis, *Mol. Cell. Biol.*, 2003, **23**, 14–25.
13 L. K. Phng and H. Gerhardt, Angiogenesis: A Team Effort Coordinated by Notch, *Dev. Cell*, 2009, **16**, 196–208.
14 I. M. Moya, L. Umans, E. Maas, P. N. G. Pereira, K. Beets, A. Francis, W. Sents, E. J. Robertson, C. L. Mummery, D. Huylebroeck and A. Zwijsen, Stalk Cell Phenotype Depends on Integration of Notch and Smad1/5 Signaling Cascades, *Dev. Cell*, 2012, **22**, 501–514.
15 J. Dufraine, Y. Funahashi and J. Kitajewski, Notch signaling regulates tumor angiogenesis by diverse mechanisms, *Oncogene*, 2008, **27**, 5132–5137.
16 D. Stenzel, C. A. Franco, S. Estrach, A. Mettouchi, D. Sauvaget, I. Rosewell, A. Schertel, H. Armer, A. Domogatskaya, S. Rodin, K. Tryggvason, L. Collinson, L. Sorokin and H. Gerhardt, Endothelial basement membrane limits tip cell formation by inducing Dll4/Notch signalling in vivo, *EMBO Rep.*, 2011, **12**, 1135–1143.
17 L. Jakobsson, C. A. Franco, K. Bentley, R. T. Collins, B. Ponsioen, I. M. Aspalter, I. Rosewell, M. Busse, G. Thurston, A. Medvinsky, S. Schulte-Merker and H. Gerhardt, Endothelial cells dynamically compete for the tip cell position during angiogenic sprouting, *Nat. Cell Biol.*, 2010, **12**, 943–953.
18 T. Hoey, W. C. Yen, F. Axelrod, J. Basi, L. Donigian, S. Dylla, M. Fitch-Bruhns, S. Lazetic, I. K. Park, A. Sato, S. Satyal, X. Wang, M. F. Clarke, J. Lewicki and A. Gurney, DLL4 Blockade Inhibits Tumor Growth and Reduces Tumor-Initiating Cell Frequency, *Cell Stem Cell*, 2009, **5**, 168–177.
19 W. C. Yen, M. M. Fischer, M. Hynes, J. Wu, E. Kim, L. Beviglia, V. P. Yeung, X. Song, A. M. Kapoun, J. Lewicki, A. Gurney, D. M. Simeone and T. Hoey, Anti-DLL4 has broad spectrum activity in pancreatic cancer dependent on targeting DLL4-notch signaling in both tumor and vasculature cells, *Clin. Cancer Res.*, 2012, **18**, 5374–5386.
20 D. Djokovic, A. Trindade, J. Gigante, M. Badenes, L. Silva, R. Liu, X. Li, M. Gong, V. Krasnoperov, P. S. Gill and A. Duarte, Combination of Dll4/Notch and Ephrin-B2/EphB4 targeted therapy is highly effective in disrupting tumor angiogenesis, *BMC Cancer*, 2010, **10**, 641.
21 J. Ridgway, G. Zhang, Y. Wu, S. Stawicki, W.-C. Liang, Y. Chanthery, J. Kowalski, R. J. Watts, C. Callahan, I. Kasman, M. Singh, M. Chien, C. Tan, J.-A. S. Hongo, F. de Sauvage, G. Plowman and M. Yan, Inhibition of Dll4 signalling inhibits tumour growth by deregulating angiogenesis, *Nature*, 2006, **444**, 1083–1087.

22 I. Noguera-Troise, C. Daly, N. J. Papadopoulos, S. Coetzee, P. Boland, N. W. Gale, H. C. Lin, G. D. Yancopoulos and G. Thurston, Blockade of Dll4 inhibits tumour growth by promoting non-productive angiogenesis, *Nature*, 2006, **444**, 1032–1037.

23 C. Roca and R. H. Adams, Regulation of vascular morphogenesis by Notch signaling Regulation of vascular morphogenesis by Notch signaling, *Genes Dev.*, 2007, **21**, 2511–2524.

24 F. Kuhnert, J. R. Kirshner and G. Thurston, Dll4-Notch signaling as a therapeutic target in tumor angiogenesis, *Vasc. Cell*, 2011, **3**, 20.

25 S. K. Ramasamy, A. P. Kusumbe, L. Wang and R. H. Adams, Endothelial Notch activity promotes angiogenesis and osteogenesis in bone, *Nature*, 2014, **507**, 376–380.

26 J. L. Li, R. C. A. Sainson, W. Shi, R. Leek, L. S. Harrington, M. Preusser, S. Biswas, H. Turley, E. Heikamp, J. A. Hainfellner and A. L. Harris, Delta-like 4 Notch ligand regulates tumor angiogenesis, improves tumor vascular function, and promotes tumor growth in vivo, *Cancer Res.*, 2007, **67**, 11244–11253.

27 Z. Xu, Z. Wang, X. Jia, L. Wang, Z. Chen, S. Wang, M. Wang, J. Zhang and M. Wu, MMGZ01, an anti-DLL4 monoclonal antibody, promotes nonfunctional vessels and inhibits breast tumor growth, *Cancer Lett.*, 2016, **372**, 118–127.

28 M. Hellström, L.-K. Phng, J. J. Hofmann, E. Wallgard, L. Coultas, P. Lindblom, J. Alva, A.-K. Nilsson, L. Karlsson, N. Gaiano, K. Yoon, J. Rossant, M. L. Iruela-Arispe, M. Kalén, H. Gerhardt and C. Betsholtz, Dll4 signalling through Notch1 regulates formation of tip cells during angiogenesis, *Nature*, 2007, **445**, 776–780.

29 S. Claxton and M. Fruttiger, Periodic Delta-like 4 expression in developing retinal arteries, *Gene Expression Patterns*, 2004, **5**, 123–127.

30 A. Stahl, K. M. Connor, P. Sapieha, J. Chen, R. J. Dennison, N. M. Krah, M. R. Seaward, K. L. Willett, C. M. Aderman, K. I. Guerin, J. Hua, C. Löfqvist, A. Hellström and L. E. H. Smith, The mouse retina as an angiogenesis model, *Invest. Ophthalmol. Visual Sci.*, 2010, **51**, 2813–2826.

31 A. Uemura, S. Kusuhara, H. Katsuta and S.-I. Nishikawa, Angiogenesis in the mouse retina: a model system for experimental manipulation, *Exp. Cell Res.*, 2006, **312**, 676–683.

32 R. F. Gariano and T. W. Gardner, Retinal angiogenesis in development and disease, *Nature*, 2005, **438**, 960–966.

33 I. W. Mak, N. Evaniew and M. Ghert, Lost in translation: animal models and clinical trials in cancer treatment, *Am. J. Transl. Res.*, 2014, **6**, 114–118.

34 C. P. Huang, J. Lu, H. Seon, A. P. Lee, L. A. Flanagan, H.-Y. Kim, A. J. Putnam and N. L. Jeon, Engineering microscale cellular niches for three-dimensional multicellular co-cultures, *Lab Chip*, 2009, **9**, 1740–1748.

35 S. Kim, M. Chung and N. L. Jeon, Three-dimensional biomimetic model to reconstitute sprouting lymphangiogenesis in vitro, *Biomaterials*, 2015, **78**, 115–128.

36 I. K. Zervantonakis, S. K. Hughes-Alford, J. L. Charest, J. S. Condeelis, F. B. Gertler and R. D. Kamm, Three-dimensional microfluidic model for tumor cell intravasation and endothelial barrier function, *Proc. Natl. Acad. Sci. U. S. A.*, 2012, **109**, 13515–13520.

37 J. S. Jeon, S. Bersini, M. Gilardi, G. Dubini, J. L. Charest, M. Moretti and R. D. Kamm, Human 3D vascularized organotypic microfluidic assays to study breast cancer cell extravasation, *Proc. Natl. Acad. Sci. U. S. A.*, 2014, 2–7.

38 Y. Zheng, Y. Sun, X. Yu, Y. Shao, P. Zhang, G. Dai and J. Fu, Angiogenesis in Liquid Tumors: An In Vitro Assay for Leukemic-Cell-Induced Bone Marrow Angiogenesis, *Adv. Healthcare Mater.*, 2016, **5**, 1014–1024.

39 S. Tao, S. Wang, S. J. Moghaddam, A. Ooi, E. Chapman, P. K. Wong and D. D. Zhang, Oncogenic KRAS confers chemoresistance by upregulating NRF2, *Cancer Res.*, 2014, **74**, 7430–7441.

40 R. Riahi, S. Wang, M. Long, N. Li, P. Y. Chiou, D. D. Zhang and P. K. Wong, Mapping photothermally induced gene expression in living cells and tissues by nanorod-locked nucleic acid complexes, *ACS Nano*, 2014, **8**, 3597–3605.

41 S. Wang, R. Riahi, N. Li, D. D. Zhang and P. K. Wong, Single Cell Nanobiosensors for Dynamic Gene Expression Profiling in Native Tissue Microenvironments, *Adv. Mater.*, 2015, **27**, 6034–6038.

42 S. Wang, J. Sun, D. D. Zhang and P. K. Wong, A nanobiosensor for dynamic single cell analysis during microvascular self-organization, *Nanoscale*, 2016, 19–22.

43 A. F. Siekmann and N. D. Lawson, Notch signalling limits angiogenic cell behaviour in developing zebrafish arteries, *Nature*, 2007, **445**, 781–784.

44 T. Iso, Y. Hamamori and L. Kedes, Notch signaling in vascular development, *Arterioscler., Thromb., Vasc. Biol.*, 2003, **23**, 543–553.

45 R. Riahi, J. Sun, S. Wang, M. Long, D. D. Zhang and P. K. Wong, Notch1-Dll4 signalling and mechanical force regulate leader cell formation during collective cell migration, *Nat. Commun.*, 2015, **6**, 6556.

46 J. J. Tung, I. W. Tattersall and J. Kitajewski, Tips, stalks, tubes: Notch-mediated cell fate determination and mechanisms of tubulogenesis during angiogenesis, *Cold Spring Harbor Perspect. Med.*, 2012, **2**, a006601.

47 S. Kim, H. Lee, M. Chung and N. L. Jeon, Engineering of functional, perfusable 3D microvascular networks on a chip, *Lab Chip*, 2013, **13**, 1489–1500.